



Title	Preparation and thermal stability of oxynitride perovskite solid solution Sr <sub>1-x</sub> La <sub>x</sub> Ta <sub>1-x</sub> Ti <sub>x</sub> O <sub>2</sub> N
Author(s)	Masubuchi, Yuji; Ohtaki, Sota; Fujii, Kotaro; Yashima, Masatomo; Higuchi, Mikio; Kikkawa, Shinichi
Citation	Journal of the European ceramic society, 40(16), 6288-6292 <a href="https://doi.org/10.1016/j.jeurceramsoc.2019.10.004">https://doi.org/10.1016/j.jeurceramsoc.2019.10.004</a>
Issue Date	2020-12
Doc URL	<a href="http://hdl.handle.net/2115/84435">http://hdl.handle.net/2115/84435</a>
Rights	©2019. This manuscript version is made available under the CC-BY-NC-ND 4.0 license <a href="http://creativecommons.org/licenses/by-nc-nd/4.0/">http://creativecommons.org/licenses/by-nc-nd/4.0/</a>
Rights(URL)	<a href="http://creativecommons.org/licenses/by-nc-nd/4.0/">http://creativecommons.org/licenses/by-nc-nd/4.0/</a>
Type	article (author version)
File Information	RE1_Manuscript-SLTTON-Manuscript.pdf



[Instructions for use](#)

Preparation and thermal stability of oxynitride perovskite solid solution  $\text{Sr}_{1-x}\text{La}_x\text{Ta}_{1-x}\text{Ti}_x\text{O}_2\text{N}$

Yuji Masubuchi<sup>1\*</sup>, Sota Ohtaki<sup>2</sup>, Kotaro Fujii<sup>3</sup>, Masatomo Yashima<sup>3</sup>, Mikio Higuchi<sup>1</sup>, and  
Shinichi Kikkawa<sup>1</sup>

Affiliations:

<sup>1</sup>Faculty of Engineering, Hokkaido University, N13 W8, Kita-ku, Sapporo 060-8628, Japan

<sup>2</sup>Graduate School of Chemical Science and Engineering, Hokkaido University, N13 W8, Kita-ku, Sapporo 060-8628, Hokkaido, Japan

<sup>3</sup>Department of Chemistry, School of Science, Tokyo Institute of Technology, 2-12-1-W4-17, O-okayama, Meguro-ku 152-8551, Tokyo, Japan

\*Corresponding Author: Y. Masubuchi; address: Faculty of Engineering, Hokkaido University.

Sapporo, 060-8628, Japan; Tel/Fax: +81-(0)11-706-6742/6740, E-mail: yuji-mas@eng.hokudai.ac.jp

## Abstract

The thermal stability of oxynitride perovskites is very important for the fabrication of their dense ceramics. In this study, a solid solution of the oxynitride perovskite  $\text{Sr}_{1-x}\text{La}_x\text{Ta}_{1-x}\text{Ti}_x\text{O}_2\text{N}$  was prepared via the ammonia nitridation of oxide precursors. The oxynitride products obtained at  $x \leq 0.2$  and  $x \geq 0.7$  had tetragonal and triclinic perovskite-type structures, respectively. A neutron diffraction study on the oxynitride product obtained at  $x = 0.2$  indicated that this tetragonal perovskite had a *cis*-type anion distribution similarly to  $\text{SrTaO}_2\text{N}$ . The tetragonal perovskite released a part of nitrogen at approximately 1000 °C in a nitrogen atmosphere while maintaining the perovskite structure at least to 1450 °C. The oxynitride perovskites at  $x \geq 0.5$  gradually decomposed to a mixture of  $\text{LaTiO}_2\text{N}$ ,  $\text{LaTiO}_3$ ,  $\text{La}(\text{OH})_3$ ,  $\text{La}_2\text{O}_3$ ,  $\text{TiN}$  and  $\text{TaO}$  above 1100 °C.

Keywords: oxynitride perovskite, ammonia nitridation, thermal stability, neutron diffraction

## Introduction

Oxynitride perovskites have attracted a lot of attention as photocatalysts and non-toxic inorganic pigments [1-5]. Oxynitride perovskites absorb visible light because they have a suitable bandgap related to a higher covalency than oxides. The anion order is an interesting structural feature that appears in oxynitride perovskites. The local ordering of nitride and oxide anions in a *cis*-type configuration has been reported for TaO<sub>4</sub>N<sub>2</sub> octahedra in SrTaO<sub>2</sub>N and BaTaO<sub>2</sub>N and for TiO<sub>4</sub>N<sub>2</sub> in LaTiO<sub>2</sub>N based on structural analysis and first principles calculations [6-8]. This ordering may affect the electrical, magnetic and especially dielectric properties of oxynitride perovskites [9, 10].

Shaping of the oxynitride perovskites, either in bulk ceramics or as thin films, is necessary for both investigations and applications of dielectric properties [11,12]. High-temperature sintering of SrTaO<sub>2</sub>N at above 1400 °C in a 0.2 MPa of nitrogen atmosphere fabricates dense oxynitride ceramics, however, the original insulating property is lost because of the partial release of nitrogen during the heating. The sintered SrTaO<sub>2</sub>N must thus be post-annealed in ammonia to recover the nitrogen content and thus the insulating property. Ceramics with a relative density of less than 85% were entirely nitrated using the post-annealing treatment [13]. The relative dielectric constant  $\epsilon_r$  ranged from 330 to 360 depending on the sintering duration at 1400 °C for the post-annealed products. For sintered

ceramics with a relative density of 95% obtained at 1450 °C, only a thin surface layer could be post-annealed. A ferroelectric response was confirmed on the annealed surface layer using piezoresponse force microscopy measurements [14].

The thermal stability of the oxynitride perovskite  $\text{LaTiO}_2\text{N}$  is very different from that of  $\text{SrTaO}_2\text{N}$ .  $\text{SrTaO}_2\text{N}$  partially releases nitrogen at approximately 950 °C in a nitrogen atmosphere while maintaining the perovskite structure as a nitrogen deficient oxynitride  $\text{SrTaO}_2\text{N}_{0.8}$  [15]. In contrast,  $\text{LaTiO}_2\text{N}$  directly decomposes into a mixture of  $\text{LaTiO}_3$ ,  $\text{La}_2\text{O}_3$ , and  $\text{TiN}$  at 1100 °C, even in a nitrogen atmosphere. Perovskite structure cannot be kept as the nitrogen deficient  $\text{LaTiO}_2\text{N}$  perovskite above 1100 °C. Therefore,  $\text{LaTiO}_2\text{N}$  is much difficult to be formed into dense ceramics in the high temperature sintering process although it has been expected to have much larger dielectric constant value than  $\text{SrTaO}_2\text{N}$  [16].

Cationic substitution in oxynitride perovskite is a promising approach for improving or tailoring their dielectric properties, similar to the cases in perovskite oxides [17,18]. Thermal stability is also modified in the solid solution to fabricate dense ceramics. In this study, a solid solution of  $\text{SrTaO}_2\text{N}$  and  $\text{LaTiO}_2\text{N}$  was prepared via the ammonia nitridation of appropriate oxide precursors. The crystal structure of the oxynitride solid solution was investigated using neutron diffraction data. The thermal stability, measured using thermogravimetry, is discussed in relation to the crystal structure.

## Experimental

The oxide precursors of  $\text{Sr}_{1-x}\text{La}_x\text{Ta}_{1-x}\text{Ti}_x\text{O}_{3.5}$  ( $0 \leq x \leq 1$ ) were prepared by firing respective mixtures of  $\text{SrCO}_3$  (99.9%, FUJIFILM Wako Pure Chemicals Co. Ltd.),  $\text{La}_2\text{O}_3$  (99.9%, Kanto Chemical Co. Inc.),  $\text{Ta}_2\text{O}_5$  (99.9%, FUJIFILM Wako Pure Chemicals Co. Ltd.), and  $\text{TiO}_2$  (99.99%, High Purity Chemicals Co. Ltd.). The starting powders were mixed by ball-milling using zirconia balls (5 mm $\phi$ ) and a pot with ethanol. Then the mixtures were heated at 1400 °C for 40 h with intermittent regrindings. The oxide precursors were nitrided on alumina boats placed in a silica tube furnace at 1000 °C for 30 h under an  $\text{NH}_3$  flow of 100 mL/min.

The phase purity was studied using powder X-ray diffraction (XRD, Ultima IV, Rigaku) with  $\text{Cu-K}\alpha$  radiation operated at 40 kV and 40 mA. The data were collected at 0.02 °/step in the range of  $20^\circ \leq 2\theta \leq 70^\circ$ . Monochromatized  $\text{Cu-K}\alpha 1$  radiation operated at 40 kV and 200 mA was also used for the powder XRD measurements (SmartLab, Rigaku) to determine the detailed crystal structure of the samples. Neutron diffraction data were obtained at beamline BL20 (iMATERIA) [19] at the Japan Proton Accelerator Research Complex (J-PARC) at 27 °C and analyzed using the software Z-Rietveld (Windows ver. 1.0.2.0) [20]. The thermal behavior of the oxynitride products was investigated using

thermogravimetry – differential thermal analysis (TG-DTA, STA2500-Regulus, Netzsch) in a nitrogen flow of 200 mL/min. The sample chamber was evacuated to 10 Pa prior to the measurements. Approximately 40 mg of the samples was heated in an alumina pan to 1450 °C at a rate of 20 °C/min.

## Results and discussion

Single phases of the oxide precursors, SrTaO<sub>3.5</sub> and LaTiO<sub>3.5</sub> were obtained at  $x = 0$  and 1, respectively as shown in Fig. 1(a). Both SrTaO<sub>3.5</sub> and LaTiO<sub>3.5</sub> have a layered perovskite structure consisting of perovskite-type slabs [21,22]. SrTaO<sub>3.5</sub> crystallizes in an orthorhombic *Cmcm* space group, whereas LaTiO<sub>3.5</sub> crystallizes in a monoclinic *P2<sub>1</sub>* due to the distortion of the TiO<sub>6</sub> octahedron. The products at  $x = 0.2$  and 0.7 were in different crystal structures similar to those of the end members of SrTaO<sub>3.5</sub> and LaTiO<sub>3.5</sub>, respectively. A mixture of the solid solutions was obtained at  $x = 0.5$ .

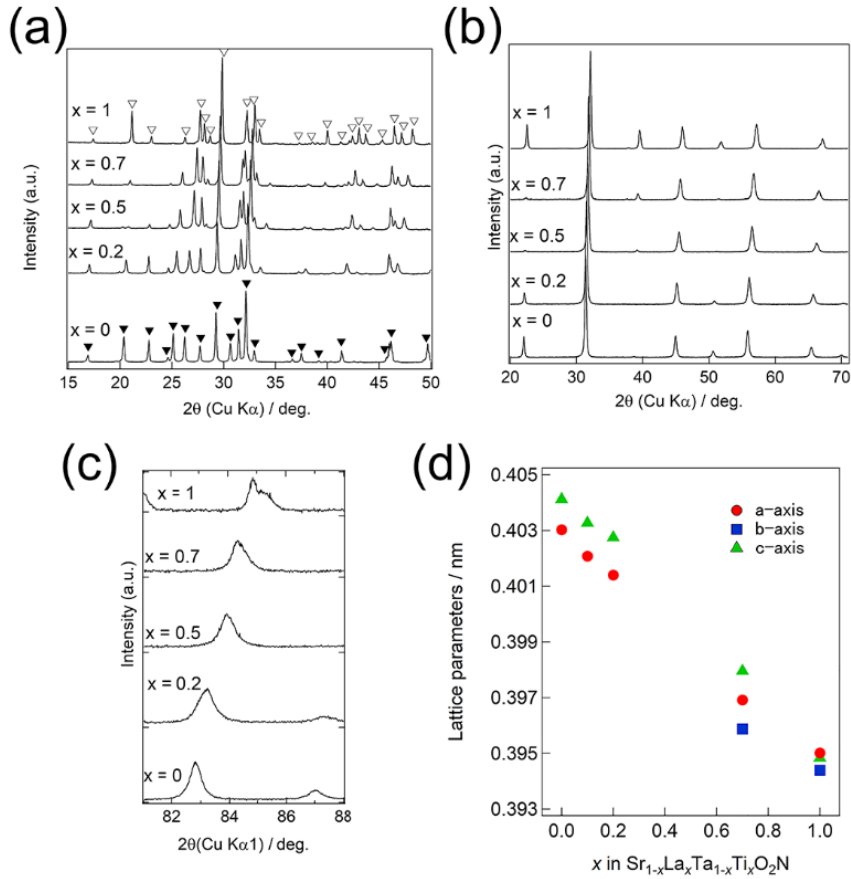


Figure 1 (a) XRD patterns for the oxide precursors of  $\text{Sr}_{1-x}\text{La}_x\text{Ta}_{1-x}\text{Ti}_x\text{O}_{3.5}$ . Diffraction lines marked with filled and open triangles correspond to  $\text{SrTaO}_{3.5}$  and  $\text{LaTiO}_{3.5}$ , respectively. (b) XRD patterns for oxynitride perovskite solid solutions, (c) magnified XRD patterns obtained using Cu- $K\alpha 1$  radiation, and (d) lattice parameters depending on  $x$  in  $\text{Sr}_{1-x}\text{La}_x\text{Ta}_{1-x}\text{Ti}_x\text{O}_2\text{N}$ . The lattice parameters are plotted as a perovskite unit to facilitate comparison between the two kinds of solid solutions.

Single phases of the perovskite structure were obtained for the entire composition range of  $\text{Sr}_{1-x}\text{La}_x\text{Ta}_{1-x}\text{Ti}_x\text{O}_2\text{N}$  after nitridation at 1000 °C in ammonia, as shown in Fig. 1(b).

The diffraction peaks of the perovskite structure shifted toward a higher diffraction angle with increasing  $x$ . Simultaneous substitution of  $\text{Sr}^{2+}$  and  $\text{Ta}^{5+}$  with  $\text{La}^{3+}$  and  $\text{Ti}^{4+}$ , which have smaller ionic sizes, shrunk the perovskite lattice [23].  $\text{SrTaO}_2\text{N}$  ( $x = 0$ ) is a tetragonal perovskite with the space group  $I4/mcm$  and  $\text{LaTiO}_2\text{N}$  ( $x = 1$ ) has a triclinic ( $I\bar{1}$ ) perovskite structure [7,16,24]. A highly symmetric perovskite structure with the space group  $Imma$  was also reported for  $\text{LaTiO}_2\text{N}$  prepared using the ammonia nitridation method with NaCl flux [25]. Powder XRD patterns for the products were measured using Cu-K $\alpha$ 1 radiation to investigate the crystal structures of the products depending on  $x$ . Figure 1(c) shows the magnified XRD patterns around a diffraction line from the 404 plane of the tetragonal  $\text{SrTaO}_2\text{N}$ . The diffraction line splits into four peaks, namely 004, 400,  $04\bar{4}$ , and  $4\bar{4}0$ , in the triclinic  $\text{LaTiO}_2\text{N}$  perovskite obtained at  $x = 1$ . A single diffraction line can be clearly observed for  $x = 0.2$  and a shoulder peak appears in higher diffraction angle side for  $x = 0.7$ . The present solid solutions were in tetragonal perovskite below  $x = 0.2$  and in triclinic perovskite above  $x = 0.7$ . It is very difficult to confirm whether the oxynitride obtained at  $x = 0.5$  is a tetragonal or triclinic perovskite from the XRD pattern shown in Fig. 1(c). Thermogravimetric analysis results and the crystalline phases of the resultant product suggest the present oxynitride obtained at  $x = 0.5$  is a mixture of these perovskite phases in different crystal structure, as discussed in later. The lattice parameters in both solid solutions linearly decrease with increasing  $x$  in the respective

compositional range of  $x \leq 0.2$  and  $x \geq 0.7$ , as shown in Fig. 1(d).

The crystal structure of the oxynitride product obtained at  $x = 0.2$  was investigated using neutron diffraction data. A tetragonal perovskite structure was refined with the space group  $I4/mcm$ , similar to the  $\text{SrTaO}_2\text{N}$ , and showed reasonable fit, as shown in Fig. 2. The refined site occupancies at the cation sites are mostly consistent with the nominal chemical composition of  $\text{Sr}_{0.8}\text{La}_{0.2}\text{Ta}_{0.8}\text{Ti}_{0.2}\text{O}_2\text{N}$  as summarized in Table 1. The oxygen/nitrogen occupancies are 0.562(2)/0.438(2) and 0.719(1)/0.281(1) for the  $4a$  and  $8h$  sites, respectively. Total nitrogen content was constrained to be 1 in the refinement. The anion distribution is similar to that in  $\text{SrTaO}_2\text{N}$ , which is assumed to have a *cis*-type configuration of nitrogen atoms, i.e., ideally  $\text{O/N}(4a) = 0.5/0.5$  and  $\text{O/N}(8h) = 0.75/0.25$  in the  $\text{TaO}_4\text{N}_2$  octahedron. The occupancies in the oxynitride solid solution obtained at  $x = 0.2$  were assumed to be  $\text{O/N}(1) = 0.5/0.5$  at the apical site ( $4a$ ) and  $\text{O/N}(2) = 0.75/0.25$  at the equatorial sites ( $8h$ ) of octahedra around  $\text{Ta}^{5+}/\text{Ti}^{4+}$ . Much larger temperature factor was obtained for the  $\text{O/N}(1)$  site similarly to the case of  $\text{SrTaO}_2\text{N}$  [7]. Bond distances in the Ta/Ti octahedra are shorter for  $x = 0.2$  because the ionic size of  $\text{Ti}^{4+}$  is smaller than that of  $\text{Ta}^{5+}$ . The substitution of  $\text{Sr}^{2+}$  with the smaller  $\text{La}^{3+}$  distorted the Ta/Ti-(O/N)<sub>6</sub> octahedral network and the bond angle  $\angle\text{O/N}(2)\text{-Ta/Ti-O/N}(2)$  decreased in the solid solution obtained at  $x = 0.2$ . The crystal structure of the oxynitride solid solution with a tetragonal perovskite structure was similar to that of  $\text{SrTaO}_2\text{N}$ .

Therefore, similar thermal stability of the oxynitride obtained at  $x = 0.2$  was expected to that for SrTaO<sub>2</sub>N.

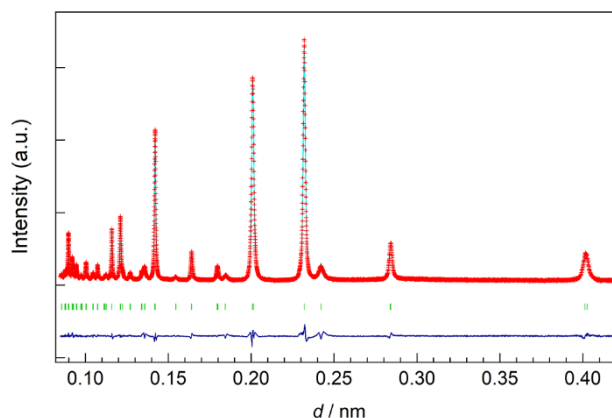


Figure 2 Neutron diffraction profile for the oxynitride perovskite Sr<sub>0.8</sub>La<sub>0.2</sub>Ta<sub>0.8</sub>Ti<sub>0.2</sub>O<sub>2</sub>N.

Table 1 Crystal parameters and reliability factors of SrTaO<sub>2</sub>N and Sr<sub>0.8</sub>La<sub>0.2</sub>Ta<sub>0.8</sub>Ti<sub>0.2</sub>O<sub>2</sub>N, which were obtained by the Rietveld analyses of neutron diffraction data taken at 27 °C.

Chemical formula	SrTaO <sub>2</sub> N	Sr <sub>0.8</sub> La <sub>0.2</sub> Ta <sub>0.8</sub> Ti <sub>0.2</sub> O <sub>2</sub> N
Crystal system	Tetragonal	Tetragonal
Space group	<i>I4/mcm</i>	<i>I4/mcm</i>
<i>a</i> / nm	0.570093(2)	0.567642(2)
<i>c</i> / nm	0.808086(9)	0.805345(5)
<i>R</i> <sub>wp</sub> / %	9.80	5.98
<i>R</i> <sub>p</sub> / %	8.03	4.58
<i>R</i> <sub>e</sub> / %	3.96	2.10
<i>S</i>	2.47	2.84
Sr/La, 4 <i>b</i> , (0, 1/2, 1/4)		
Site occupancies Sr/La	1/0	0.809(3)/0.191(3)
<i>U</i> <sub>iso</sub> * / 10 <sup>2</sup> nm <sup>2</sup>	0.00078(1)	0.0124(1)
Ta/Ti, 4 <i>c</i> , (1/2, 1/2, 0)		
Site occupancies Ta/Ti	1/0	0.805(3)/0.195(3)
<i>U</i> <sub>iso</sub> * / 10 <sup>2</sup> nm <sup>2</sup>	0.0044(1)	0.0034(1)
O/N(1), 4 <i>a</i> , (0, 0, 1/4)		
Site occupancies O/N	0.551(8)/0.449(8)	0.562(2)/0.438(2)
<i>U</i> <sub>iso</sub> * / 10 <sup>2</sup> nm <sup>2</sup>	0.0289(3)	0.0427(2)
O/N(2), 8 <i>h</i> , ( <i>x</i> , <i>x</i> -1/2, 0)		

$x$	0.7689(8)	0.7718(2)
Site occupancies O/N	0.725(3)/0.275(3)	0.719(1)/0.281(1)
$U_{\text{iso}}^* / 10^2 \text{ nm}^2$	0.0083(1)	0.0105(1)

\*the anisotropic displacement parameters are shown in Table 2.

Table 2 Room-temperature anisotropic parameters ( $\times 10^2 \text{ nm}^2$ ) of  $\text{SrTaO}_2\text{N}$  and  $\text{Sr}_{0.8}\text{La}_{0.2}\text{Ta}_{0.8}\text{Ti}_{0.2}\text{O}_2\text{N}$ .

Chemical formula	atom	site	$U_{11}=U_{22}$	$U_{33}$	$U_{12}$	$U_{23}=U_{13}$
$\text{SrTaO}_2\text{N}$	Sr	4b	0.0011(2)	0.0221(5)	0	0
	Ta	4c	0.0061(2)	0.0086(5)	0	0
	O/N1	4a	0.0433(3)	0.0260(5)	0	0
	O/N2	8h	0.0089(1)	0.0073(3)	0.0106(2)	0
$\text{Sr}_{0.8}\text{La}_{0.2}\text{Ta}_{0.8}\text{Ti}_{0.2}\text{O}_2\text{N}$	Sr/La	4b	0.0146(2)	0.0068(4)	0	0
	Ta/Ti	4c	0.0043(1)	0.0016(2)	0	0
	O/N1	4a	0.0435(3)	0.0235(4)	0	0
	O/N2	8h	0.0068(1)	0.0267(3)	0.0059(1)	0

Table 3 Selected bond distances and angles in  $\text{SrTaO}_2\text{N}$  and  $\text{Sr}_{0.8}\text{La}_{0.2}\text{Ta}_{0.8}\text{Ti}_{0.2}\text{O}_2\text{N}$  refined based on neutron diffraction data.

	$\text{SrTaO}_2\text{N}$	$\text{Sr}_{0.8}\text{La}_{0.2}\text{Ta}_{0.8}\text{Ti}_{0.2}\text{O}_2\text{N}$
Bond distances / nm		
Ta/Ti – O/N(1)	0.202022(3)	0.201336(3)
Ta/Ti – O/N(2)	0.2021(5)	0.20145(15)
Angles / °		
O/N(2)-Ta/Ti-O/N(2)	171.4(3)	170.03(12)

The thermal behavior of the oxynitride solid solutions was examined using TG/DTA in a nitrogen atmosphere. The results are shown in Fig. 3. As reported in our previous paper [15], the weight loss of  $\text{SrTaO}_2\text{N}$  started at approximately 1000 °C. The weight loss of 0.8 wt% corresponds to a partial release of nitrogen from  $\text{SrTaO}_2\text{N}$ , creating nitrogen-deficient

$\text{SrTaO}_2\text{N}_{0.8}$ . Weight loss below 600 °C is attributed to a release of adsorbates, such as  $\text{CO}_2$  and the humidity in ambient atmosphere. The product heated at 1450 °C after the partial nitrogen release was dark green in color and maintained the perovskite structure having a trace amount of TaO as shown in Fig. 4(a). The first weight loss started at approximately 850 °C for the  $\text{LaTiO}_2\text{N}$  perovskite. The second weight loss, corresponding to a decomposition reaction, was observed at above 1100 °C. The product was a mixture of  $\text{LaTiO}_2\text{N}$ ,  $\text{LaTiO}_3$ ,  $\text{La}(\text{OH})_3$ , TiN, and  $\text{La}_2\text{O}_3$ , as shown in Fig. 4(e). In the oxynitride solid solution obtained at  $x = 0.2$ , the first weight loss started at a lower temperature of 900 °C than the temperature in  $\text{SrTaO}_2\text{N}$  and the second weight loss does not appear below 1450 °C. The first weight loss amount was about 1.0 wt%, which is larger than that for  $\text{SrTaO}_2\text{N}$ . It corresponds to a chemical composition of  $\text{Sr}_{0.8}\text{La}_{0.2}\text{Ta}_{0.8}\text{Ti}_{0.2}\text{O}_2\text{N}_{0.79}$  assuming that the Sr, Ta, La, Ti, and O content did not change during heat treatment. The product maintained the perovskite structure, similar to  $\text{SrTaO}_2\text{N}$ , and had a small amount of the impurity phase TaO. A large second weight loss at above 1100 °C was observed for the oxynitride obtained at  $x = 0.7$ . The product was contaminated with  $\text{La}_2\text{O}_3$  and TiN suggesting that the perovskite phase decomposed. For  $x = 0.5$ , a very small second weight loss appeared at above 1200 °C and the product contained a TiN impurity phase, as shown in Fig. 4(c). The oxynitride solid solutions obtained at  $x = 0$  and 0.2 both had a tetragonal perovskite structure with the space

group  $I4/mcm$  and high thermal stability. Only a part of nitrogen was released from the oxynitrides, which maintained their perovskite structure, becoming nitrogen-deficient perovskites. It has been suggested that the partial loss of nitrogen leads to the formation of a more isotropic perovskite structure, which loses the local ordering in the  $cis\text{-TaO}_4\text{N}_2$  octahedra with nitrogen loss during heating [15].

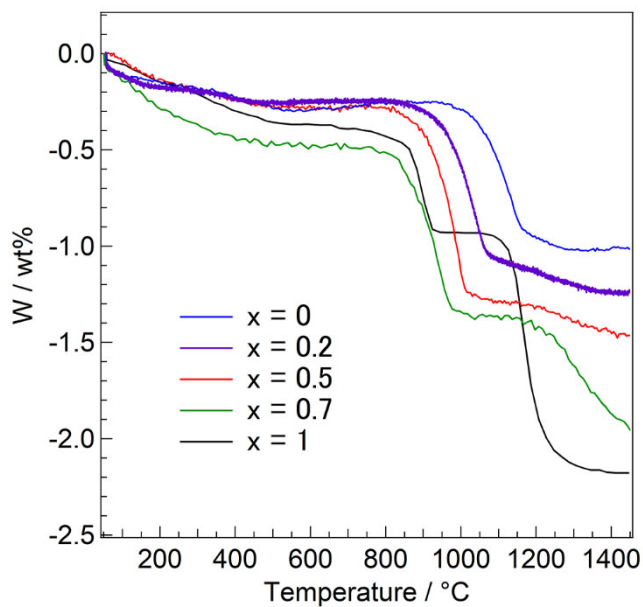


Figure 3 TG curves for oxynitride perovskites  $\text{Sr}_{1-x}\text{La}_x\text{Ta}_{1-x}\text{Ti}_x\text{O}_2\text{N}$  in  $\text{N}_2$  atmosphere.

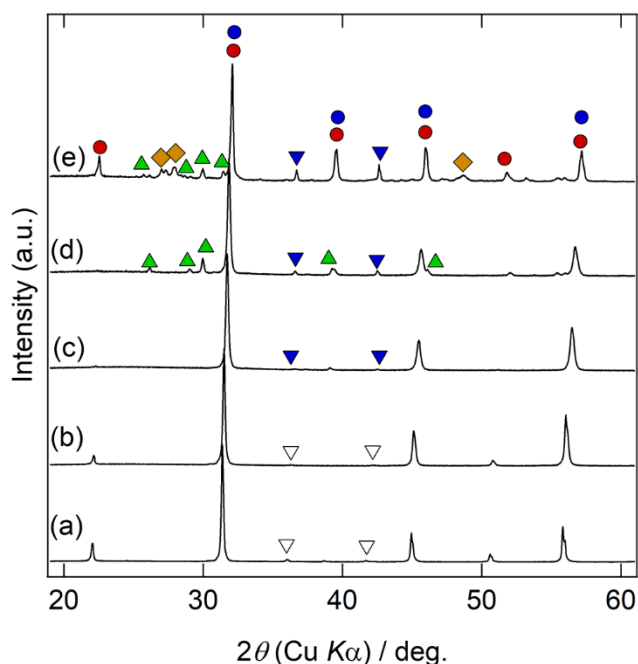


Figure 4 XRD patterns for oxynitride perovskites  $\text{Sr}_{1-x}\text{La}_x\text{Ta}_{1-x}\text{Ti}_x\text{O}_2\text{N}$  after TG measurement at 1450 °C in  $\text{N}_2$  flow. (a)  $x = 0$ , (b) 0.2, (c) 0.5, (d) 0.7 and (e) 1. Blue circles, red circles, yellow diamonds, green triangles, blue and open inverse triangles were assigned for  $\text{LaTiO}_2\text{N}$ ,  $\text{LaTiO}_3$ ,  $\text{La}(\text{OH})_3$ ,  $\text{La}_2\text{O}_3$ ,  $\text{TiN}$  and  $\text{TaO}$ , respectively.

Sintering behavior was studied on the series of the oxynitride solid solution at above 1400 °C in a 0.2 MPa  $\text{N}_2$  atmosphere. Black sintered ceramics were obtained on the oxynitrides at  $x = 0$  and 0.2. They were nitrogen-deficient perovskites. Relative density was 85% at  $x = 0.2$  and 80% at  $x = 0$  on the ceramics obtained at 1800 °C for 3 hours. The oxynitrides obtained at  $x = 0.5, 0.7$ , and 1 did not sinter well because they decomposed at high temperature even under the 0.2 MPa  $\text{N}_2$  atmosphere. The slightly higher relative density

in the oxynitride obtained at  $x = 0.2$  might be attributed to an enhanced diffusion in the oxynitride related to the thermal decomposition in solid solution in higher  $x$ -value. The sintered ceramics were electrically conductive because of the partial nitrogen loss accompanied by a reduction of  $Ta^{5+}/Ti^{4+}$ . Further investigation on the recovery of the nitrogen content to the stoichiometric composition should be performed to study the dielectric properties.

## **Conclusion**

Two kinds of perovskite phases were obtained in a  $Sr_{1-x}La_xTa_{1-x}Ti_xO_2N$  solid solution. One was a tetragonal perovskite with the space group  $I4/mcm$  similar to  $SrTaO_2N$  in the compositional range below  $x = 0.2$ . It released a part of nitrogen while maintaining the perovskite structure at above  $1450\text{ }^\circ\text{C}$  even in nitrogen atmosphere. The *cis*-type anion configuration in the tetragonal oxynitride obtained at  $x = 0.2$  was clarified using a structural analysis based on neutron diffraction data. It has a possibility to obtain its ceramic body. The other was a triclinic perovskite above  $x = 0.7$ . The perovskite structure was easily decomposed in high temperature above  $1100\text{ }^\circ\text{C}$ .

## **Acknowledgements**

This work was supported by the JSPS Grant-in-Aid for Scientific Research on Innovative Areas "Mixed Anion" (grant nos. JP16H06438, JP16H06439, JP16H06440). Neutron diffraction experiments at J-PARC were performed with the approval of Proposal nos. 2017A0023 and 2017A0064. Powder XRD using Cu-Ka1 radiation were carried out with a SmartLab diffractometer (Rigaku) supported by "Material Analysis and Structure Analysis Open Unit (MASAOU)" of Hokkaido University.

## References

- [1] K. Maeda, K. Domen, New non-oxide photocatalysts designed for overall water splitting under visible light, *J. Phys. Chem. C* 111 (2007) 7851-7861.
- [2] S.G. Ebbinghaus, H.P. Abicht, R. Dronskowski, T. Muller, A. Reller, A. Weidenkaff, Perovskite-related oxynitrides - Recent developments in synthesis, characterisation and investigations of physical properties, *Prog. Solid State Chem.* 37 (2009) 173-205.
- [3] K. Hibino, M. Yashima, T. Oshima, K. Fujii, K. Maeda, Structures, electron density and characterization of novel photocatalysts,  $(\text{BaTaO}_2\text{N})_{1-x}(\text{SrWO}_2\text{N})_x$  solid solutions, *Dalton Trans.* 46 (2017) 14947-14956.
- [4] M. Jansen, H.P. Letschert, Inorganic yellow-red pigments without toxic metals, *Nature* 404 (2000) 980-982.

- [5] F. Tessier, P. Maillard, F. Chevire, K. Domen, S. Kikkawa, Optical properties of oxynitride powders, *J. Ceram. Soc. Jpn.* 117 (2009) 1-5.
- [6] M. Yang, J. Oro-Sole, J.A. Rodgers, A.B. Jorge, A. Fuertes, J.P. Attfield, Anion order in perovskite oxynitrides, *Nature Chem.* 3 (2011) 47-52.
- [7] Y.R. Zhang, T. Motohashi, Y. Masubuchi, S. Kikkawa, Local anionic ordering and anisotropic displacement in dielectric perovskite SrTaO<sub>2</sub>N, *J. Ceram. Soc. Jpn.* 119 (2011) 581-586.
- [8] Y. Hinuma, H. Moriwake, Y.R. Zhang, T. Motohashi, S. Kikkawa, I. Tanaka, First-principles study on relaxor-type ferroelectric behavior without chemical inhomogeneity in BaTaO<sub>2</sub>N and SrTaO<sub>2</sub>N, *Chem. Mater.* 24 (2012) 4343-4349.
- [9] A. Fuertes, Synthesis and properties of functional oxynitrides - from photocatalysts to CMR materials, *Dalton Trans.* 39 (2010) 5942-5948.
- [10] J.P. Attfield, Principles and applications of anion order in solid oxynitrides, *Cryst. Growth Des.* 13 (2013) 4623-4629.
- [11] Y. Masubuchi, S.K. Sun, S. Kikkawa, Processing of dielectric oxynitride perovskites for powder, ceramics, compacts, and thin films, *Dalton Trans.* 44 (2015) 10570-10581.
- [12] S. Jacq, C. Le Paven, L. Le Gendre, R. Benzerga, F. Chevire, F. Tessier, A. Sharaiha, Deposition and dielectric characterization of strontium and tantalum-based oxide and

oxynitride perovskite thin films, *Solid State Sci.* 54 (2016) 22-29.

[13] S.K. Sun, Y.R. Zhang, Y. Masubuchi, T. Motohashi, and S. Kikkawa, Additive sintering, postannealing, and dielectric properties of SrTaO<sub>2</sub>N, *J. Am. Ceram. Soc.* 97 (2014) 1023-1027.

[14] S. Kikkawa, S.K. Sun, Y. Masubuchi, Y. Nagamine, T. Shibahara, Ferroelectric response induced in cis-type anion ordered SrTaO<sub>2</sub>N oxynitride perovskite, *Chem. Mater.* 28 (2016) 1312-1317.

[15] D. Chen, D. Habu, Y. Masubuchi, S. Torii, T. Kamiyama, S. Kikkawa, Partial nitrogen loss in SrTaO<sub>2</sub>N and LaTiO<sub>2</sub>N oxynitride perovskites, *Solid State Sci.*, 54 (2016) 2-6.

[16] D. Habu, Y. Masubuchi, S. Torii, T. Kamiyama, S. Kikkawa, Crystal structure study of dielectric oxynitride perovskites La<sub>1-x</sub>Sr<sub>x</sub>TiO<sub>2+x</sub>N<sub>1-x</sub> (x = 0, 0.2), *J. Solid State Chem.* 237 (2016) 254-257.

[17] J.F. Scott, C.A.P. de Araujo, Ferroelectric memories, *Science* 246 (1989) 1400-1405.

[18] Y. Saito, H. Takao, T. Tani, T. Nonoyama, K. Takatori, T. Homma, T. Nagaya, M. Nakamura, Lead-free piezoceramics, *Nature*, 432 (2004) 84-87.

[19] T. Ishigaki, A. Hoshikawa, M. Yonemura, T. Morishima, T. Kamiyama, R. Oishi, K. Aizawa, T. Sakuma, Y. Tomota, M. Arai, M. Hayashi, K. Ebata, Y. Takano, K. Komatsuzaki, H. Asano, Y. Takano, T. Kasao, IBARAKI materials design diffractometer (iMATERIA) – Versatile

neutron diffractometer at J-PARC, Nucl. Instr. Methods Phys. Res. A 600 (2009) 189-191.

[20] R. Oishi-Tomiyasu, M. Yonemura, T. Morishima, A. Hoshikawa, S. Torii, T. Ishigaki, T. Kamiyama, Application of matrix decomposition algorithms for singular matrices to the Pawley method in Z-Rietveld, J. Appl. Crystallogr. 45 (2012) 299–308.

[21] N. Ishizawa, F. Marumo, T. Kawamura, M. Kimura, Compounds with perovskite-type slabs. II. The crystal structure of  $\text{Sr}_2\text{Ta}_2\text{O}_7$ , Acta Crystallogr. B32 (1976) 2564-2566.

[22] M. Gasperi, Ditungstate de lanthane, Acta Crystallogr. B31 (1975) 2129-2130.

[23] R.D. Shannon, Revised effective ionic radii and systematic studies of interatomic distances in halides and chalcogenides, Acta Crystallogr. A32 (1976) 751-767.

[24] D. Logvinovich, L. Bocher, D. Sheptyakov, R. Figi, S.G. Ebbinghaus, R. Aguiar, M.H. Aguirre, A. Reller, A. Weidenkaff, Microstructure, surface composition and chemical stability of partly ordered  $\text{LaTiO}_2\text{N}$ , Solid State Sci. 11 (2009) 1513-1519.

[25] M. Yashima, M. Saito, H. Nakano, T. Takata, K. Ogisu, K. Domen, Imma perovskite-type oxynitride  $\text{LaTiO}_2\text{N}$ : structure and electron density, Chem. Commun. 46 (2010) 4704-4706.